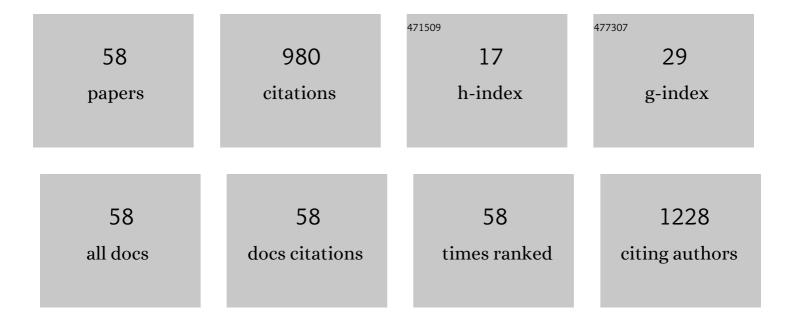
List of Publications by Year in descending order

Source: https://exaly.com/author-pdf/8406966/publications.pdf Version: 2024-02-01



ΥΠ ΖΗΛΝΟ

#	Article	IF	CITATIONS
1	The red blood cell damage after long-term exposure to shear stresses. Journal of Artificial Organs, 2022, , 1.	0.9	0
2	Air pollutant dispersion around high-rise buildings due to roof emissions. Building and Environment, 2022, 219, 109215.	6.9	5
3	CFD-based analysis of urban haze-fog dispersion—A preliminary study. Building Simulation, 2021, 14, 365-375.	5.6	10
4	Comparison of LBM and FVM in the estimation of LAD stenosis. Proceedings of the Institution of Mechanical Engineers, Part H: Journal of Engineering in Medicine, 2021, 235, 1058-1068.	1.8	1
5	Promotion of the Wound Healing of <i>in vivo</i> Rabbit Wound Infected With Methicillin-Resistant <i>Staphylococcus aureus</i> Treated by a Cold Atmospheric Plasma Jet. IEEE Transactions on Plasma Science, 2021, 49, 2329-2339.	1.3	6
6	A Novel Method for Estimating the Dosage of Cold Atmospheric Plasmas in Plasma Medical Applications. Applied Sciences (Switzerland), 2021, 11, 11135.	2.5	1
7	MP-PIC simulation of blood cell movement through a LAD with high stenosis. Powder Technology, 2020, 361, 448-454.	4.2	6
8	Flow resistance coefficient analysis of left anterior descending artery stenosis: A preliminary study. Proceedings of the Institution of Mechanical Engineers, Part H: Journal of Engineering in Medicine, 2020, 234, 100-109.	1.8	4
9	Numerical simulation of the mixing process in a soft elastic reactor with bionic contractions. Chemical Engineering Science, 2020, 220, 115623.	3.8	14
10	Estimation of the turbulent viscous shear stress in a centrifugal rotary blood pump by the large eddy particle image velocimetry method. Journal of Hydrodynamics, 2020, 32, 486-496.	3.2	3
11	Effect of pollutant source location on air pollutant dispersion around a high-rise building. Applied Mathematical Modelling, 2020, 81, 582-602.	4.2	24
12	Multiphase particle-in-cell simulation in severe internal carotid artery stenosis. Powder Technology, 2019, 358, 62-67.	4.2	11
13	Promotion of Wound Healing of Genetic Diabetic Mice Treated by a Cold Atmospheric Plasma Jet. IEEE Transactions on Plasma Science, 2019, 47, 4848-4860.	1.3	19
14	The Impact of Erythrocytes Injury on Blood Flow in Bionic Arteriole with Stenosis Segment. Processes, 2019, 7, 372.	2.8	2
15	Fluorescent reconstitution on deposition of PM _{2.5} in lung and extrapulmonary organs. Proceedings of the National Academy of Sciences of the United States of America, 2019, 116, 2488-2493.	7.1	105
16	Mixing in a softâ€elastic reactor (SER): A simulation study. Canadian Journal of Chemical Engineering, 2019, 97, 676-686.	1.7	19
17	Study of wind flow over a 6†m cube using improved delayed detached Eddy simulation. Journal of Wind Engineering and Industrial Aerodynamics, 2018, 179, 463-474.	3.9	16
18	Ceruloplasmin in Parkinson's disease and the nonmotor symptoms. Brain and Behavior, 2018, 8, e00995.	2.2	14

#	Article	IF	CITATIONS
19	Investigation of cold atmospheric plasma treatment in polydimethylsiloxane microfluidic devices with a transmural method. Journal of Physics Condensed Matter, 2018, 30, 384001.	1.8	0
20	Experimental study and numerical simulation of periodic bubble formation at submerged micron-sized nozzles with constant gas flow rate. Chemical Engineering Science, 2017, 168, 1-10.	3.8	31
21	Hemolysis in a continuous-flow ventricular assist device with/without chamfer. Advances in Mechanical Engineering, 2017, 9, 168781401769789.	1.6	7
22	Air pollutant dispersion around high-rise buildings under different angles of wind incidence. Journal of Wind Engineering and Industrial Aerodynamics, 2017, 167, 51-61.	3.9	38
23	Hemodynamic analysis of intracranial aneurysms using phase-contrast magnetic resonance imaging and computational fluid dynamics. Acta Mechanica Sinica/Lixue Xuebao, 2017, 33, 472-483.	3.4	2
24	Lactic Dehydrogenase in the In Vitro Evaluation of Hemolytic Properties of Ventricular Assist Device. Artificial Organs, 2017, 41, E274-E284.	1.9	7
25	Evaluation of the carotid artery stenosis based on minimization of mechanical energy loss of the blood flow. Proceedings of the Institution of Mechanical Engineers, Part H: Journal of Engineering in Medicine, 2016, 230, 1051-1058.	1.8	10
26	Wake-induced vibration of a small cylinder in the wake of a large cylinder. Ocean Engineering, 2016, 113, 75-89.	4.3	20
27	Characteristics of air pollutant dispersion around a high-rise building. Environmental Pollution, 2015, 204, 280-288.	7.5	51
28	Blood flow reduction of covered small side branches after flow diverter treatment: A computational fluid hemodynamic quantitative analysis. Journal of Biomechanics, 2015, 48, 895-898.	2.1	14
29	Large eddy simulation of flow around an inclined finite square cylinder. Journal of Wind Engineering and Industrial Aerodynamics, 2015, 146, 172-184.	3.9	63
30	Computational fluid dynamics–discrete element method analysis of the onset of scour around subsea pipelines. Applied Mathematical Modelling, 2015, 39, 7611-7619.	4.2	25
31	Computational Hemodynamics Analysis of Intracranial Aneurysms Treated with Flow Diverters: Correlation with Clinical Outcomes. American Journal of Neuroradiology, 2014, 35, 136-142.	2.4	71
32	Haemodynamic analysis of vessel remodelling in STA-MCA bypass for Moyamoya disease and its impact on bypass patency. Journal of Biomechanics, 2014, 47, 1800-1805.	2.1	18
33	A fluid–structure interaction study using patient-specific ruptured and unruptured aneurysm: The effect of aneurysm morphology, hypertension and elasticity. Journal of Biomechanics, 2013, 46, 2402-2410.	2.1	41
34	The influence of elastic upstream artery length on fluid–structure interaction modeling: A comparative study using patient-specific cerebral aneurysm. Medical Engineering and Physics, 2013, 35, 1377-1384.	1.7	9
35	Analysis of restenosis after carotid artery stenting: Preliminary results using computational fluid dynamics based on three-dimensional angiography. Journal of Clinical Neuroscience, 2013, 20, 1582-1587.	1.5	11
36	Investigation of intracranial aneurysm hemodynamics following flow diverter stent treatment. Medical Engineering and Physics, 2013, 35, 608-615.	1.7	64

#	Article	IF	CITATIONS
37	A comparison of estimation methods for computational fluid dynamics outflow boundary conditions using patient-specific carotid artery. Proceedings of the Institution of Mechanical Engineers, Part H: Journal of Engineering in Medicine, 2013, 227, 663-671.	1.8	5
38	Proposition of an outflow boundary approach for carotid artery stenosis CFD simulation. Computer Methods in Biomechanics and Biomedical Engineering, 2013, 16, 488-494.	1.6	20
39	Propose a Wall Shear Stress Divergence to Estimate the Risks of Intracranial Aneurysm Rupture. Scientific World Journal, The, 2013, 2013, 1-8.	2.1	8
40	Investigation of image segmentation methods for intracranial aneurysm haemodynamic research. , 2013, , .		0
41	Mean Arterial Pressure Required for Maintaining Patency of Extracranial-to-Intracranial Bypass Grafts. Neurosurgery, 2012, 71, 826-832.	1.1	8
42	Flow resistance analysis of extracranial-to-intracranial (EC–IC) vein bypass. Journal of Biomechanics, 2012, 45, 1400-1405.	2.1	12
43	A comparison of medical image segmentation methods for cerebral aneurysm computational hemodynamics. , 2011, , .		9
44	Statistical particle stress in aeolian sand movement-derivation and validation. Powder Technology, 2011, 209, 147-151.	4.2	10
45	CFD analysis of pneumatic conveying in a double-tube-socket (DTS®) pipe. Applied Mathematical Modelling, 2010, 34, 3085-3097.	4.2	10
46	Experimental and numerical study on power consumptions in a double-tube-socket pneumatic conveying system. Powder Technology, 2010, 204, 268-272.	4.2	12
47	Study on peak overpressure and flame propagation speed of gas deflagration in the tube with obstacles. Science China Technological Sciences, 2010, 53, 1847-1854.	4.0	2
48	CFD-DEM simulation of three-dimensional aeolian sand movement. Science China: Physics, Mechanics and Astronomy, 2010, 53, 1306-1318.	5.1	11
49	CFD study of a sudden-expanding coal combustor using Euler–Euler and Euler–Lagrange models. Fuel, 2010, 89, 3643-3649.	6.4	4
50	Sand storms: CFD analysis of Reynolds stress and collision stress of particles near sand bed. Particuology, 2010, 8, 325-331.	3.6	4
51	CFD analysis of thermodynamic cycles in a pulse tube refrigerator. Cryogenics, 2010, 50, 743-749.	1.7	27
52	Numerical and experimental investigation on the prevention of CO deflagration. Journal of Loss Prevention in the Process Industries, 2009, 22, 169-175.	3.3	2
53	Numerical analysis of blast furnace hearth inner profile by using CFD and heat transfer model for different time periods. International Journal of Heat and Mass Transfer, 2008, 51, 186-197.	4.8	36
54	A Methodology for Blast Furnace Hearth Inner Profile Analysis. Journal of Heat Transfer, 2007, 129, 1729-1731.	2.1	7

#	Article	IF	CITATIONS
55	Studies of the effect of a coal concentrator on NO formation in swirling coal combustion. International Journal of Heat and Mass Transfer, 2006, 49, 421-426.	4.8	11
56	Simulation of coal combustion by AUSM turbulence-chemistry char combustion model and a full two-fluid model. Fuel, 2005, 84, 1798-1804.	6.4	12
57	Simulation of swirling coal combustion using a full two-fluid model and an AUSM turbulence-chemistry modelâ~†. Fuel, 2003, 82, 1001-1007.	6.4	27
58	Aortic valve opening in mock-loop with continuous-flow left ventricular assist device. International Journal of Artificial Organs, 0, , 039139882211118.	1.4	1